

LEARNING TO DIAGNOSE WITH LSTM RECURRENT NEURAL NETWORKS

Zachary C. Lipton *

Department of Computer Science and Engineering
 University of California, San Diego
 La Jolla, CA 92093, USA
 zlipton@cs.ucsd.edu

David C. Kale †

Department of Computer Science
 University of Southern California
 Los Angeles, CA 90089
 dkale@usc.edu

Charles Elkan

Department of Computer Science and Engineering
 University of California, San Diego
 La Jolla, CA 92093, USA
 elkan@cs.ucsd.edu

Randall Wetzel

Laura P. and Leland K. Whittier Virtual PICU
 Children’s Hospital Los Angeles
 Los Angeles, CA 90027
 rwetzel@chla.usc.edu

ABSTRACT

Clinical medical data, especially in the intensive care unit (ICU), consist of multivariate time series of observations. For each patient visit (or *episode*), sensor data and lab test results are recorded in the patient’s Electronic Health Record (EHR). While potentially containing a wealth of insights, the data is difficult to mine effectively, owing to varying length, irregular sampling and missing data. Recurrent Neural Networks (RNNs), particularly those using Long Short-Term Memory (LSTM) hidden units, are powerful and increasingly popular models for learning from sequence data. They effectively model varying length sequences and capture long range dependencies. We present the first study to empirically evaluate the ability of LSTMs to recognize patterns in multivariate time series of clinical measurements. Specifically, we consider multilabel classification of diagnoses, training a model to classify 128 diagnoses given 13 frequently but irregularly sampled clinical measurements. First, we establish the effectiveness of a simple LSTM network for modeling clinical data. Then we demonstrate a straightforward and effective training strategy in which we replicate targets at each sequence step. Trained only on raw time series, our models outperform several strong baselines on a wide variety of metrics, and nearly match the performance of a multilayer perceptron trained on hand-engineered features, establishing the usefulness of LSTMs for modeling medical data. The best LSTM model accurately classifies many diagnoses, including diabetic ketoacidosis (F1 score of .933), status asthmaticus (.653), and scoliosis (.582).

1 INTRODUCTION

Time series data comprised of clinical measurements, as recorded by caregivers in the pediatric intensive care unit (PICU), constitute an abundant and largely untapped source of medical insights. Potential uses of such data include classifying diagnoses accurately, predicting length of stay, predicting future illness, and predicting mortality. However, besides the difficulty of acquiring data, several obstacles stymie machine learning research with clinical time series. Episodes vary in length, with stays ranging from just a few hours to multiple months. Observations, which include sensor data, vital signs, lab test results, and subjective assessments, are sampled irregularly and plagued by missing values (Marlin et al., 2012). Additionally, long-term time dependencies complicate learning with many algorithms. Lab results that, taken together, might imply a particular diagnosis may be separated by days or weeks. Other examples include delays separating onsets of diseases from the

* Author website: <http://zacklipton.com>

† Author website: <http://www-scf.usc.edu/~dkale/>

appearance of symptoms. For example, symptoms of acute respiratory distress syndrome may not appear until 24-48 hours after lung injury (Mason et al., 2010).

Recurrent Neural Networks (RNNs), in particular those based on Long Short-Term Memory (LSTM) (Hochreiter & Schmidhuber, 1997), model varying-length sequential data, achieving state-of-the-art results for problems spanning natural language processing, image captioning, handwriting recognition, and genomic analysis (Auli et al., 2013; Sutskever et al., 2014; Vinyals et al., 2014; Karpathy & Fei-Fei, 2014; Liwicki et al., 2007; Graves et al., 2009; Pollastri et al., 2002; Vohradský, 2001; Xu et al., 2007). LSTMs can capture long range dependencies and nonlinear dynamics. Some sequence models, such as Markov models, conditional random fields, and Kalman filters, deal with sequential data but are ill-equipped to learn long-range dependencies. Other models require domain knowledge or feature engineering, offering less chance for serendipitous discovery. In contrast, neural networks learn representations and can discover unforeseen structure.

This paper presents the first empirical study applying LSTMs to classify diagnoses given multivariate PICU time series. Specifically, we formulate the problem as multilabel classification, since diagnoses are not mutually exclusive. Our examples are clinical episodes, each consisting of 13 frequently but irregularly sampled time series of clinical measurements, including body temperature, heart rate, diastolic and systolic blood pressure, and blood glucose, among others. Associated with each patient are a subset of 429 diagnosis codes. As some are rare, we focus on the 128 most common codes, classifying each episode with one or more diagnoses.

Because LSTMs have never been used in this setting, we first verify their utility. We establish a set of strong baselines, and verify that our proposed LSTM architecture can beat a linear classifier, even when the linear model is trained on hand-engineered features and the LSTM is trained on raw time series. We then test a straightforward but novel *target replication* strategy for recurrent neural networks, inspired by the *deep supervision* technique of Lee et al. (2014) for training convolutional neural networks. We compose our optimization objective as a convex combination of the loss at the final sequence step and the mean of the losses over *all* sequence steps. Comparing against other neural networks, the LSTM with target replication surpasses the performance of a MultiLayer Perceptron (MLP) trained on raw time series, and nearly matches an MLP trained on the expert features.

Experiments demonstrate that target replication with a well-tuned mixing parameter acts as a powerful regularizer, improving performance on all evaluation metrics and reducing overfitting. Finally, we evaluate the efficacy of using additional information in the patient’s chart as auxiliary outputs, a technique previously used with feedforward nets (Caruana et al., 1996). We show that this too regularizes the model and that in combination with target replication, it yields higher performance on some metrics.

2 RELATED WORK

Our research sits at the intersection of LSTMs, medical informatics, and multilabel classification, three mature fields, each with a long history and rich body of research. While we cannot possibly do justice to all three, we highlight the most relevant works below.

2.1 LSTM RNNs

LSTMs were originally introduced in Hochreiter & Schmidhuber (1997), following a long line of research into RNNs for sequence learning. Notable earlier work includes Elman (1990), which first used back-propagation through time to train recurrent neural networks to perform supervised machine learning. The design of modern LSTM memory cells has remained close to the original, with the commonly used addition of forget gates (Gers et al., 2000b) (which we use), and peep-hole connections (Gers et al., 2000a) (which we do not use). The connectivity pattern among multiple LSTM layers in our models follows the architecture described by Graves (2013). Pascanu et al. (2013) explores other mechanisms by which an RNN could be made *deep*. Surveys of the literature include Graves (2012), a thorough dissertation on sequence labeling with RNNs, De Mulder et al. (2015), which surveys natural language applications, and Lipton et al. (2015), which provides a broad overview of RNNs for sequence learning, focusing on modern applications.

2.2 NEURAL NETWORKS FOR MEDICAL DATA

Neural networks have been applied to medical problems and data for at least 20 years (Caruana et al., 1996; Baxt, 1995), although we know of no work on applying LSTMs to multivariate clinical time series of the type we analyze here. Several papers have applied RNNs to physiologic signals, including electrocardiograms (Silipo & Marchesi, 1998; Amari & Cichocki, 1998; Übeyli, 2009) and glucose measurements (Tresp & Briegel, 1998). RNNs have also been used for prediction problems in genomics (Pollastri et al., 2002; Xu et al., 2007; Vohradský, 2001). Multiple recent papers apply modern deep learning techniques (but not RNNs) to modeling psychological conditions (Dabek & Caban, 2015), head injuries (Rughani et al., 2010), and Parkinson’s disease (Hammerla et al., 2015). Recently, feedforward networks have been applied to medical time series in sliding window fashion to classify cases of gout, leukemia (Lasko et al., 2013), and critical illness (Che et al., 2015).

2.3 NEURAL NETWORKS FOR MULTILABEL CLASSIFICATION

Only a few published papers apply LSTMs to multilabel classification tasks, all of which, to our knowledge, are outside of the medical context. Liu et al. (2014) formulates music composition as a multilabel classification task, using sigmoidal output units. Most recently, Yeung et al. (2015) uses LSTM networks with multilabel outputs to recognize actions in videos. While we could not locate any published papers using LSTMs for multilabel classification in the medical domain, several papers use feedforward nets for this task. One of the earliest papers to investigate multi-task neural networks modeled risk in pneumonia patients (Caruana et al., 1996). More recently, Che et al. (2015) formulated diagnosis as multilabel classification using a sliding window multilayer perceptron.

2.4 MACHINE LEARNING FOR CLINICAL TIME SERIES

Neural network methodology aside, a growing body of research applies machine learning to temporal clinical data for tasks including artifact removal (Aleks et al., 2009; Quinn et al., 2009), early detection and prediction (Stanculescu et al., 2014; Henry et al., 2015), and clustering and subtyping (Marlin et al., 2012; Schulam et al., 2015). Many recent papers use models with latent factors to capture nonlinear dynamics in clinical time series and to discover meaningful representations of health and illness. Gaussian processes and related techniques have proved popular because they can directly handle irregular sampling and encode prior knowledge via choice of covariance functions between time steps and across variables (Marlin et al., 2012; Ghassemi et al., 2015). Saria et al. (2010) combined a hierarchical dirichlet process with autoregressive models to infer latent disease “topics” in the heart rate signals of premature babies. Quinn et al. (2009) used linear dynamical systems with latent switching variables to model physiologic events like bradycardias. Citing inspiration from deep learning, Stanculescu et al. (2015) proposed models with a second “layer” of latent factors to capture correlations between latent states.

2.5 KEY DIFFERENCES

Our experiments show that LSTMs can accurately classify multivariate time series of clinical measurements, a topic not addressed in any prior work. Additionally, while some papers use LSTMs for multilabel classification, ours is the first to address this problem in the medical context. Moreover, for classifying varying length sequences with fixed length output vectors, this paper is the first, to our knowledge, to demonstrate the efficacy of a target replication strategy, achieving both faster training and better generalization.

3 DATA DESCRIPTION

Our experiments use a collection of anonymized clinical time series extracted from the EHR system at Children’s Hospital LA (Marlin et al., 2012; Che et al., 2015) as part of an IRB-approved study. The data consists of 10,401 PICU episodes, each a multivariate time series of 13 variables: diastolic and systolic blood pressure, peripheral capillary refill rate, end-tidal CO₂, fraction of inspired O₂, Glasgow coma scale, blood glucose, heart rate, pH, respiratory rate, blood oxygen saturation, body temperature, and urine output. Episodes vary in length from 12 hours to several months.

Each episode is associated with zero or more diagnostic labels from an in-house taxonomy used for research and billing, similar to codes from the *Ninth Revision of the International Classification of Diseases* (ICD-9) (World Health Organization, 2004). The dataset contains 429 distinct labels indicating a variety of conditions, such as acute respiratory distress, congestive heart failure, seizures, renal failure, and sepsis. Because many of the diagnoses are rare, we focus on the most common 128, each of which occurs more than 50 times in the dataset.

Each example consists of irregularly sampled multivariate time series with both missing values and, occasionally, missing variables. We resample all time series to an hourly rate, taking the mean measurement within each one hour window. We use forward- and back-filling to fill gaps created by the window-based resampling. When a single variable’s time series is missing entirely, we impute a clinically normal value, as defined by domain experts. These procedures make reasonable assumptions about clinical practice: many variables are recorded at rates proportional to how quickly they change, and when a variable is absent, it is often because clinicians believed it to be normal and chose not to measure it. Nonetheless, these procedures are not appropriate in all settings. Back-filling, for example, passes information from the future backwards. This is acceptable for classifying entire episodes (as we do) but not for forecasting. Finally, we rescale all variables to $[0, 1]$, using ranges defined by clinical experts. Specifically, we use published tables of normal values from large population studies to correct for differences in heart rate, respiratory rate, (Fleming et al., 2011) and blood pressure (NHBPEP Working Group 2004) due to age and gender.

4 METHODS

In this work, we are interested in recognizing diagnoses and, more broadly, the observable physiologic characteristics of patients, a task generally termed *phenotyping* (Oellrich et al., 2015). We cast the problem of phenotyping clinical time series as multilabel classification. Given a series of observations $\mathbf{x}^{(1)}, \dots, \mathbf{x}^{(T)}$, we learn a classifier to generate hypotheses $\hat{\mathbf{y}}$ of the true labels \mathbf{y} . Here, t indexes sequence steps, and for any example, T stands for the length of the sequence. Our proposed LSTM RNN uses memory cells with forget gates (Gers et al., 2000b) but without peephole connections (Gers et al., 2003). As output, we use a fully connected layer atop the highest LSTM layer followed by an element-wise sigmoid activation function, because our problem is multilabel. We use *log loss* as the loss function at each output.

The following equations give the update for a layer of memory cells $\mathbf{h}_l^{(t)}$ where $\mathbf{h}_{l-1}^{(t)}$ stands for the previous layer at the same sequence step (could be a previous LSTM layer or the input layer $\mathbf{x}^{(t)}$) and $\mathbf{h}_l^{(t-1)}$ stands for the same layer at the previous sequence step:

$$\begin{aligned} \mathbf{g}_l^{(t)} &= \phi(W_l^{\text{gx}} \mathbf{h}_{l-1}^{(t)} + W_l^{\text{gh}} \mathbf{h}_l^{(t-1)} + \mathbf{b}_l^{\text{g}}) \\ \mathbf{i}_l^{(t)} &= \sigma(W_l^{\text{ix}} \mathbf{h}_{l-1}^{(t)} + W_l^{\text{ih}} \mathbf{h}_l^{(t-1)} + \mathbf{b}_l^{\text{i}}) \\ \mathbf{f}_l^{(t)} &= \sigma(W_l^{\text{fx}} \mathbf{h}_{l-1}^{(t)} + W_l^{\text{fh}} \mathbf{h}_l^{(t-1)} + \mathbf{b}_l^{\text{f}}) \\ \mathbf{o}_l^{(t)} &= \sigma(W_l^{\text{ox}} \mathbf{h}_{l-1}^{(t)} + W_l^{\text{oh}} \mathbf{h}_l^{(t-1)} + \mathbf{b}_l^{\text{o}}) \\ \mathbf{s}_l^{(t)} &= \mathbf{g}_l^{(t)} \odot \mathbf{i}_l^{(t)} + \mathbf{s}_l^{(t-1)} \odot \mathbf{f}_l^{(t)} \\ \mathbf{h}_l^{(t)} &= \phi(\mathbf{s}_l^{(t)}) \odot \mathbf{o}_l^{(t)}. \end{aligned}$$

In these equations, σ stands for an element-wise application of the *sigmoid (logistic)* function, ϕ stands for an element-wise application of the *tanh* function and \odot is the Hadamard (element-wise) product. The input, output, and forget gates are denoted by \mathbf{i} , \mathbf{o} , and \mathbf{f} respectively, while \mathbf{g} is the input node and has a *tanh* activation.

4.1 LSTM ARCHITECTURES FOR MULTILABEL CLASSIFICATION

We explore several recurrent neural network architectures for multilabel classification of time series. The first and simplest (Figure 1) passes over all inputs in chronological order, generating outputs only at the final sequence step. In this approach, we only have output $\hat{\mathbf{y}}$ at the final sequence step, at

which our loss function is the average of the losses at each output node. Thus the loss calculated at a single sequence step is the average of *log loss* calculated separately on each label.

$$\text{loss}(\hat{\mathbf{y}}, \mathbf{y}) = \frac{1}{|L|} \sum_{l=1}^{|L|} -(y_l \cdot \log(\hat{y}_l) + (1 - y_l) \cdot \log(1 - \hat{y}_l)).$$

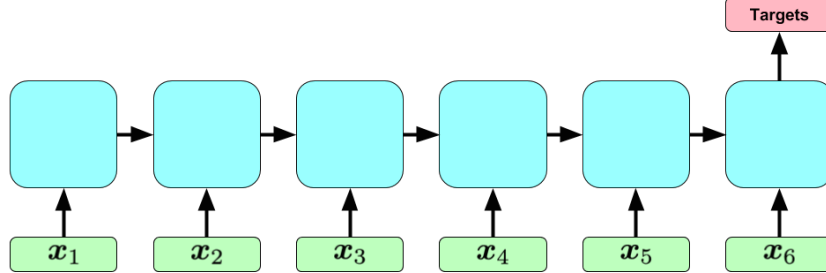


Figure 1: A simple RNN model for multilabel classification. Green rectangles represent inputs. The recurrent hidden layers separating input and output are represented with a single blue rectangle. The red rectangle represents targets.

4.2 SEQUENTIAL TARGET REPLICATION

One problem with the simple approach is that the network must learn to pass information across many sequence steps in order to affect the output. We attack this problem by replicating our static targets at each sequence step (Figure 2), providing a local error signal at each step. This approach is inspired by the deep supervision technique that Lee et al. (2014) apply to convolutional nets. This technique is especially sensible in our case because we expect the model to predict accurately even if the sequence were truncated by a small amount. The approach differs from Lee et al. (2014) because we use the same output weights to calculate $\hat{y}^{(t)}$ for all t . Further, we use this target replication to generate output at each sequence step, but not at each hidden layer.

For the model with target replication, we generate an output $\hat{y}^{(t)}$ at every sequence step. Our loss is then a convex combination of the final loss and the average of the losses over all steps:

$$\alpha \cdot \frac{1}{T} \sum_{t=1}^T \text{loss}(\hat{y}^{(t)}, \mathbf{y}^{(t)}) + (1 - \alpha) \cdot \text{loss}(\hat{y}^{(T)}, \mathbf{y}^{(T)})$$

where T is the total number of sequence steps and $\alpha \in [0, 1]$ is a hyper-parameter which determines the relative importance of hitting these intermediary targets. At prediction time, we take only the output at the final step. In our experiments, networks using target replication outperformed those with a loss applied only at the final sequence step.

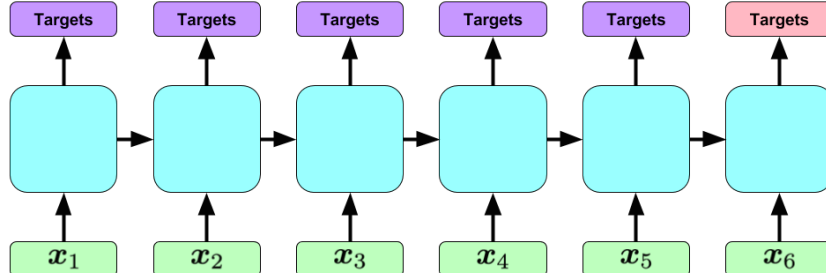


Figure 2: An RNN classification model with *target replication*. The primary target (depicted in red) at the final step is used at prediction time, but during training, the model back-propagates errors from the intermediate targets (purple) at every sequence step.

5 AUXILIARY OUTPUT TRAINING

Recall that our initial data contained 429 diagnostic labels but that our task is to predict only 128. Given the well-documented successes of multitask learning with shared representations and feed-forward networks, we wish to train a stronger model by using the remaining 301 labels or other information in the patient’s chart, such as diagnostic categories, as auxiliary targets (Caruana et al., 1996). These additional targets serve as regularizers in that the model aims to minimize the loss on the labels of interest but must learn representations that also minimize loss on the auxiliary targets (Figure 3).

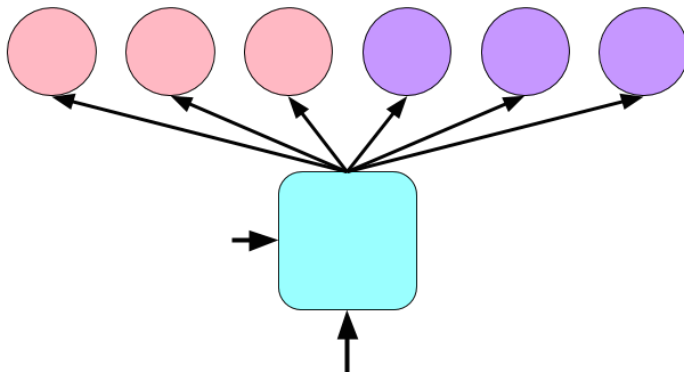


Figure 3: Our dataset contains many labels. For our task, a subset of 128 are of interest (depicted in red). Our *Auxiliary Output* neural network makes use of extra labels as additional training targets (depicted in purple). At inference time we generate predictions for only the labels of interest.

6 EXPERIMENTS

The training details are as follows. All models are trained on 80% of the data and tested on 10%. The remaining 10% is used as a validation set. We train the network using stochastic gradient descent (SGD) with momentum. To combat exploding gradients, we experimented with scaling the norm of the gradient, truncating back-propagation to 500 sequence steps, and using ℓ_2^2 weight decay, which also serves as a regularizer. The final network used all three techniques. Additionally, we found that target replication not only helps to learn faster but also reduces overfitting. In our final network, we use ℓ_2^2 regularization strength of 10^{-6} and target replication with $\alpha = 0.6$, hyper-parameters which were chosen using validation data. Our final network uses 2 hidden layers and 64 nodes per layer, an architecture also determined on the validation set.

6.1 MULTILABEL EVALUATION METHODOLOGY

We report micro- and macro-averaged versions of Area Under the ROC Curve (AUC). By micro AUC we mean a single AUC computed on flattened \hat{Y} and Y matrices, whereas we calculate macro AUC by averaging each per-label AUC. The blind classifier achieves 0.5 macro AUC but can exceed 0.5 on micro AUC by predicting labels in descending order by base rate. Additionally, we report micro- and macro-averaged F1 score. Similarly, micro is reported on flattened matrices and macro is an average over the individual label performances. F1 metrics require a thresholding strategy, and here we select thresholds based upon validation set performance. We refer to Lipton et al. (2014) for an analysis of the strengths and weaknesses of each type of multilabel F-score and a characterization of optimal thresholds.

Finally, we report *precision at 10*, which captures the fraction of true diagnoses among the model’s top 10 predictions, with a best possible score of 0.2281 on the test split of this data set because there are on average 2.281 diagnoses per patient. While F1 and AUC are both useful for determining the relative quality of a classifier’s predictions, neither is tailored to a real-world application. Thus, we consider a medically plausible use case to motivate this more interpretable metric: generating a short

list of the 10 most probable diagnoses. If we could create a high recall, moderate precision list of 10 likely diagnoses, it could be a valuable hint-generation tool. Further, testing for only the 10 most probable conditions is much more realistic than testing for all conditions.

6.2 BASELINE CLASSIFIERS

We provide results for a *base rate* model that predicts diagnoses in descending order by incidence to provide a minimum performance baseline. We also report the performance of logistic regression, which is widely used in clinical research, training a separate classifier for each diagnosis and choosing an overall ℓ_2 regularization penalty on the validation set. For a much stronger baseline, we train a multilabel MLP with rectified linear activations, dropout of 0.5, and 3 hidden layers and 300 hidden nodes, hyper-parameters chosen based on validation set performance. Each baseline is tested with two sets of inputs: raw time series and hand-engineered features. For raw time series, we use the first and last six hours. This provides classifiers with temporal information about changes in patient state from admission to discharge within a fixed-size input, as required by all baselines. We find this works better than providing the first or last 12 hours. Our hand-engineered features are inspired by those used in state-of-the-art severity of illness scores (Pollack et al., 1996) and capture extremes (e.g., maximum), central tendencies (e.g., mean), variability, and trends. Such features have previously been shown to be effective for these data (Marlin et al., 2012; Che et al., 2015).

6.3 RESULTS

LSTM models with two layers of 64 hidden units and trained with target replication (LSTM-TR) perform best among models using only raw time series as inputs. Target replication improves performance over simple LSTMs on all metrics, accelerating learning and reducing overfitting. Back-propagating error from outputs at every step, target replication provides local targets to guide training, which may aid the LSTM-TR in modeling long-term dependencies. **Table 1** shows summary results for all models. All three TR models achieve micro and macro AUCs of over 0.84 and 0.78, respectively. **Table 2** shows the LSTM’s predictive performance for five critical care diagnoses with the highest F1 scores. Full per-diagnosis results can be found in **Appendix A**.

LSTMs with target replication outperform both the linear baseline and also the MLP trained on a fixed window. Our model also outperforms a linear model trained on hand-engineered features, but is outperformed by an MLP trained on the hand-engineered features. We find these results encouraging, and there is ample reason to believe the LSTM could be improved even further. To begin with, given the superiority of the LSTM on raw time series, we could develop an LSTM model which combines the raw time series with the hand-engineered ones to form a yet stronger model.

Overall classification performance for 128 ICU phenotypes using raw time series features					
Model	Micro AUC	Macro AUC	Micro F1	Macro F1	Prec. at 10
Base Rate	0.7128	0.5	0.1346	0.0343	0.0788
Logistic Regression, First 6 + Last 6	0.8074	0.7218	0.2221	0.1029	0.1021
MLP, First 6 + Last 6	0.8375	0.7770	0.2698	0.1286	0.1096
ML-LSTM	0.8300	0.7625	0.2611	0.1323	0.1093
ML-LSTM, AuxOut (Diagnoses)	0.8353	0.7703	0.2577	0.1333	0.1099
ML-LSTM, AuxOut (Categories)	0.8316	0.7671	0.2654	0.1251	0.1082
ML-LSTM-TR	0.8450	0.7842	0.2800	0.1365	0.1165
ML-LSTM-TR, AuxOut (Diagnoses)	0.8461	0.7926	0.2701	0.1414	0.1153
ML-LSTM-TR, AuxOut (Categories)	0.8461	0.7887	0.2818	0.1411	0.1136
Overall classification performance for 128 ICU phenotypes using hand-engineered features					
Logistic Regression	0.8286	0.7550	0.2515	0.1254	0.1111
MLP	0.8525	0.7990	0.2917	0.1468	0.1157

Table 1: Results on performance metrics calculated across all labels. *TR* indicates target replication, and *AuxOut* indicates *auxiliary outputs*. *AuxOut (Diagnoses)* uses the extra diagnosis codes and *AuxOut (Categories)* uses diagnostic category information as additional targets during training.

Auxiliary outputs improved performance for most metrics, and reduced overfitting, but not as effectively as target replication. Additionally, these gains came at the cost of slower training: the

auxiliary output models required more epochs, especially when using the 301 remaining diagnoses. This may be due in part to severe class imbalance in the extra labels. For many of these labels it may take an entire epoch just to learn that they are occasionally nonzero.

Best 5 Labels measured by F1				
Label	F1	AUC	Precision	Recall
Diabetes mellitus with ketoacidosis	0.9333	0.9966	1.0000	0.8750
Asthma, unspecified with status asthmaticus	0.6531	0.9228	0.6667	0.6400
Scoliosis, idiopathic	0.5824	0.8259	0.6496	0.5278
Neoplasm, brain, unspecified	0.5401	0.8237	0.4961	0.5926
Acute respiratory distress syndrome	0.5000	0.9475	0.4286	0.6000

Table 2: Results on performance metrics calculated on the 5 labels with highest F1.

7 DISCUSSION

Our results indicate that LSTM RNNs, especially with target replication, can successfully classify diagnoses of critical care patients given clinical time series data. Our experiments demonstrate a clear advantage over all linear baselines and over traditional feedforward architectures applied to raw time series. However, this is only a first step in this line of research. Recognizing current diagnoses given only sensor data demonstrates that LSTMs can capture meaningful signal, but ultimately we would like to accurately predict unknown conditions and events, including outcomes such as mortality and treatment responses. In this work we used diagnostic labels without timestamps, but we are working to obtain time-stamped diagnoses, which would enable us to train models to perform early diagnosis by predicting future conditions. On the strength of these results, we are currently extending this work to a larger PICU data set with a richer set of measurements, including treatments and medications.

On the methodological side, we would like to both improve and better exploit the capabilities of LSTMs. Results from speech recognition have shown that LSTMs shine in comparison to other models using raw features. In the clinical setting, LSTMs may allow us to exploit previously difficult to mine sources of data while minimizing the preprocessing and feature engineering required. In contrast, our current data preparation pipeline removes valuable structure and information from clinical time series that could be exploited by an LSTM. For example, our forward- and back-filling imputation strategies discard useful information about when each observations is recorded. Imputing normal values for missing time series ignores the meaningful distinction between truly normal and missing measurements. Also, our window-based resampling procedure reduces the variability of more frequently measured vital signs (e.g., heart rate).

In future work, we plan to introduce indicator variables to allow the LSTM to distinguish actual from missing or imputed measurements. Additionally the flexibility of the LSTM architecture should enable us to eliminate age-based corrections and to incorporate non-sequential inputs, such as age, weight, and height (or even hand-engineered features), into predictions. Other next steps in this direction include developing LSTM architectures to directly handle missing values and irregular sampling. We also are encouraged by the success of target replication and plan to explore other variants of this technique and to apply it to other domains and tasks. Additionally, we acknowledge that there remains a debate about the interpretability of neural networks when applied to complex medical problems. We are developing methods to interpret the representations learned by LSTMs in order to better expose patterns of health and illness to clinical users. We also hope to make practical use of the distributed representations of patients for tasks including patient similarity search.

8 ACKNOWLEDGEMENTS

Zachary C. Lipton was supported by the Division of Biomedical Informatics at the University of California, San Diego, via training grant (T15LM011271) from the NIH/NLM. David Kale was supported by the Alfred E. Mann Innovation in Engineering Doctoral Fellowship. The VPICU was supported by grants from the Laura P. and Leland K. Whittier Foundation. We acknowledge NVIDIA Corporation for Tesla K40 GPU hardware donation and Professors Julian McAuley and Greg Ver Steeg for their support and advice.

REFERENCES

Aleks, Norm, Russell, Stuart J, Madden, Michael G, Morabito, Diane, Staudemayer, Kristan, Cohen, Mitchell, and Manley, Geoffrey T. Probabilistic detection of short events, with application to critical care monitoring. In *Advances in Neural Information Processing Systems*, pp. 49–56, 2009.

Amari, Shun-ichi and Cichocki, Andrzej. Adaptive blind signal processing-neural network approaches. *Proceedings of the IEEE*, 86(10):2026–2048, 1998.

Auli, Michael, Galley, Michel, Quirk, Chris, and Zweig, Geoffrey. Joint language and translation modeling with recurrent neural networks. In *EMNLP*, volume 3, pp. 0, 2013.

Baxt, W.G. Application of artificial neural networks to clinical medicine. *The Lancet*, 346(8983): 1135–1138, 1995. ISSN 0140-6736.

Caruana, Rich, Baluja, Shumeet, Mitchell, Tom, et al. Using the future to “sort out” the present: Rankprop and multitask learning for medical risk evaluation. *Advances in neural information processing systems*, pp. 959–965, 1996.

Che, Zhengping, Kale, David C., Li, Wenzhe, Bahadori, Mohammad Taha, and Liu, Yan. Deep computational phenotyping. In *Proceedings of the 21th ACM SIGKDD International Conference on Knowledge Discovery and Data Mining*, KDD ’15, pp. 507–516, New York, NY, USA, 2015. ACM. ISBN 978-1-4503-3664-2. doi: 10.1145/2783258.2783365. URL <http://doi.acm.org/10.1145/2783258.2783365>.

Dabek, Filip and Caban, Jesus J. A neural network based model for predicting psychological conditions. In *Brain Informatics and Health*, pp. 252–261. Springer, 2015.

De Mulder, Wim, Bethard, Steven, and Moens, Marie-Francine. A survey on the application of recurrent neural networks to statistical language modeling. *Computer Speech & Language*, 30(1): 61–98, 2015.

Elman, Jeffrey L. Finding structure in time. *Cognitive Science*, 14(2):179–211, 1990.

Fleming, Susannah, Thompson, Matthew, Stevens, Richard, Heneghan, Carl, Plddemann, Annette, Maconochie, Ian, Tarassenko, Lionel, and Mant, David. Normal ranges of heart rate and respiratory rate in children from birth to 18 years: A systematic review of observational studies. *Lancet*, pp. 1011–1018, 2011.

Gers, Felix, Schmidhuber, Jürgen, et al. Recurrent nets that time and count. In *Neural Networks, 2000. IJCNN 2000, Proceedings of the IEEE-INNS-ENNS International Joint Conference on*, volume 3, pp. 189–194. IEEE, 2000a.

Gers, Felix A., Schmidhuber, Jürgen, and Cummins, Fred. Learning to forget: Continual prediction with LSTM. *Neural Computation*, 12(10):2451–2471, 2000b.

Gers, Felix A., Schraudolph, Nicol N., and Schmidhuber, Jürgen. Learning precise timing with lstm recurrent networks. *The Journal of Machine Learning Research*, 3:115–143, 2003.

Ghassemi, Marzyeh, Pimentel, Marco AF, Naumann, Tristan, Brennan, Thomas, Clifton, David A, Szolovits, Peter, and Feng, Mengling. A multivariate timeseries modeling approach to severity of illness assessment and forecasting in ICU with sparse, heterogeneous clinical data. In *Proc. Twenty-Ninth AAAI Conf. on Artificial Intelligence*, 2015.

Graves, Alex. *Supervised sequence labelling with recurrent neural networks*, volume 385. Springer, 2012.

Graves, Alex. Generating sequences with recurrent neural networks. *arXiv preprint arXiv:1308.0850*, 2013.

Graves, Alex, Liwicki, Marcus, Fernández, Santiago, Bertolami, Roman, Bunke, Horst, and Schmidhuber, Jürgen. A novel connectionist system for unconstrained handwriting recognition. *Pattern Analysis and Machine Intelligence, IEEE Transactions on*, 31(5):855–868, 2009.

Hammerla, Nils Y, Fisher, James M, Andras, Peter, Rochester, Lynn, Walker, Richard, and Plötz, Thomas. Pd disease state assessment in naturalistic environments using deep learning. In *Proc. Twenty-Ninth AAAI Conf. on Artificial Intelligence*, 2015.

Henry, Katharine E, Hager, David N, Pronovost, Peter J, and Saria, Suchi. A targeted real-time early warning score (trewscore) for septic shock. *Science Translational Medicine*, 7(299):299ra122–299ra122, 2015.

Hochreiter, Sepp and Schmidhuber, Jürgen. Long short-term memory. *Neural Computation*, 9(8):1735–1780, 1997.

Karpathy, Andrej and Fei-Fei, Li. Deep visual-semantic alignments for generating image descriptions. *arXiv preprint arXiv:1412.2306*, 2014.

Lasko, Thomas A., Denny, Joshua C., and Levy, Mia A. Computational phenotype discovery using unsupervised feature learning over noisy, sparse, and irregular clinical data. *PLoS ONE*, 8(6):e66341, 06 2013. doi: 10.1371/journal.pone.0066341.

Lee, Chen-Yu, Xie, Saining, Gallagher, Patrick, Zhang, Zhengyou, and Tu, Zhuowen. Deeply-supervised nets. *arXiv preprint arXiv:1409.5185*, 2014.

Lipton, Zachary C, Elkan, Charles, and Narayanaswamy, Balakrishnan. Optimal thresholding of classifiers to maximize f1 measure. In *Machine Learning and Knowledge Discovery in Databases*, pp. 225–239. Springer, 2014.

Lipton, Zachary C., Berkowitz, John, and Elkan, Charles. A critical review of recurrent neural networks for sequence learning. *arXiv preprint arXiv:1506.00019*, 2015.

Liu, I, Ramakrishnan, Bhiksha, et al. Bach in 2014: Music composition with recurrent neural network. *arXiv preprint arXiv:1412.3191*, 2014.

Liwicki, Marcus, Graves, Alex, Bunke, Horst, and Schmidhuber, Jürgen. A novel approach to on-line handwriting recognition based on bidirectional long short-term memory networks. In *Proc. 9th Int. Conf. on Document Analysis and Recognition*, volume 1, pp. 367–371, 2007.

Marlin, Ben M., Kale, David C., Khemani, Robinder G., and Wetzel, Randall C. Unsupervised pattern discovery in electronic health care data using probabilistic clustering models. In *IHI*, 2012.

Mason, Robert J., Broaddus, V. Courtney, Martin, Thomas, King Jr., Talmadge E., Schraufnagel, Dean, Murray, John F., and Nadel, Jay A. *Murray and Nadel's textbook of respiratory medicine: 2-volume set*. Elsevier Health Sciences, 2010.

National High Blood Pressure Education Program Working Group on Children and Adolescents. The fourth report on the diagnosis, evaluation, and treatment of high blood pressure in children and adolescents. *Pediatrics*, 114:555–576, 2004.

Oellrich, Anika, Collier, Nigel, Groza, Tudor, Rebholz-Schuhmann, Dietrich, Shah, Nigam, Bodenreider, Olivier, Boland, Mary Regina, Georgiev, Ivo, Liu, Hongfang, Livingston, Kevin, Luna, Augustin, Mallon, Ann-Marie, Manda, Prashanti, Robinson, Peter N., Rustici, Gabriella, Simon, Michelle, Wang, Liqin, Winnenburg, Rainer, and Dumontier, Michel. The digital revolution in phenotyping. *Briefings in Bioinformatics*, 2015. doi: 10.1093/bib/bbv083.

Pascanu, Razvan, Gulcehre, Caglar, Cho, Kyunghyun, and Bengio, Yoshua. How to construct deep recurrent neural networks. *arXiv preprint arXiv:1312.6026*, 2013.

Pollack, M. M., Patel, K. M., and Ruttimann, U. E. *PRISM III: an updated Pediatric Risk of Mortality score*. *Critical Care Medicine*, 24(5):743–752, 1996.

Pollastri, Gianluca, Przybylski, Darisz, Rost, Burkhard, and Baldi, Pierre. Improving the prediction of protein secondary structure in three and eight classes using recurrent neural networks and profiles. *Proteins: Structure, Function, and Bioinformatics*, 47(2):228–235, 2002.

Quinn, John, Williams, Christopher KI, McIntosh, Neil, et al. Factorial switching linear dynamical systems applied to physiological condition monitoring. *Pattern Analysis and Machine Intelligence, IEEE Transactions on*, 31(9):1537–1551, 2009.

Rughani, Anand I., Dumont, Travis M., Lu, Zhenyu, Bongard, Josh, Horgan, Michael A., Penar, Paul L., and Tranmer, Bruce I. Use of an artificial neural network to predict head injury outcome: clinical article. *Journal of neurosurgery*, 113(3):585–590, 2010.

Saria, Suchi, Koller, Daphne, and Penn, Anna. Learning individual and population level traits from clinical temporal data. In *Proc. Neural Information Processing Systems (NIPS), Predictive Models in Personalized Medicine workshop*. Citeseer, 2010.

Schulam, Peter, Wigley, Fredrick, and Saria, Suchi. Clustering longitudinal clinical marker trajectories from electronic health data: Applications to phenotyping and endotype discovery. In *Twenty-Ninth AAAI Conference on Artificial Intelligence*, 2015.

Silipo, Rosaria and Marchesi, Carlo. Artificial neural networks for automatic ecg analysis. *Signal Processing, IEEE Transactions on*, 46(5):1417–1425, 1998.

Stanculescu, Ioan, Williams, Christopher K, Freer, Yvonne, et al. Autoregressive hidden markov models for the early detection of neonatal sepsis. *Biomedical and Health Informatics, IEEE Journal of*, 18(5):1560–1570, 2014.

Stanculescu, Ioan, Williams, Christopher KI, and Freer, Yvonne. A hierarchical switching linear dynamical system applied to the detection of sepsis in neonatal condition monitoring. 2015.

Sutskever, Ilya, Vinyals, Oriol, and Le, Quoc VV. Sequence to sequence learning with neural networks. In *Advances in Neural Information Processing Systems*, pp. 3104–3112, 2014.

Tresp, Volker and Briegel, Thomas. A solution for missing data in recurrent neural networks with an application to blood glucose prediction. In Jordan, M.I., Kearns, M.J., and Solla, S.A. (eds.), *Advances in Neural Information Processing Systems 10*, pp. 971–977. MIT Press, 1998.

Übeyli, Elif Derya. Combining recurrent neural networks with eigenvector methods for classification of ecg beats. *Digital Signal Processing*, 19(2):320–329, 2009.

Vinyals, Oriol, Toshev, Alexander, Bengio, Samy, and Erhan, Dumitru. Show and tell: A neural image caption generator. *arXiv preprint arXiv:1411.4555*, 2014.

Vohradský, Jiří. Neural network model of gene expression. *The FASEB Journal*, 15(3):846–854, 2001.

World Health Organization. *International statistical classification of diseases and related health problems*, volume 1. World Health Organization, 2004.

Xu, Rui, Wunsch II, Donald, and Frank, Ronald. Inference of genetic regulatory networks with recurrent neural network models using particle swarm optimization. *IEEE/ACM Transactions on Computational Biology and Bioinformatics (TCBB)*, 4(4):681–692, 2007.

Yeung, Serena, Russakovsky, Olga, Jin, Ning, Andriluka, Mykhaylo, Mori, Greg, and Fei-Fei, Li. Every moment counts: Dense detailed labeling of actions in complex videos. *arXiv preprint arXiv:1507.05738*, 2015.

Appendices

A PER DIAGNOSIS RESULTS

Condition	Classifier Performance on Each Diagnostic Code, Sorted by F1			
	ML-LSTM-TR, AuxOut (Diagnoses)		MLP, First 6 + Last 6	
	F1	AUC	F1	AUC
Diabetes mellitus with ketoacidosis	0.9333	0.9966	0.8750	0.9960
Asthma, unspecified with status asthmaticus	0.6531	0.9228	0.5263	0.9252
Scoliosis, idiopathic	0.5824	0.8259	0.5277	0.8135
Neoplasm, brain, unspecified	0.5401	0.8237	0.4646	0.8343
Acute respiratory distress syndrome	0.5000	0.9475	0.3107	0.9597
Developmental delay	0.4294	0.8284	0.3980	0.7968
Acute respiratory failure	0.4167	0.7871	0.3266	0.7553
Shock, septic	0.3826	0.8309	0.3146	0.8160
Acute renal failure	0.3404	0.8405	0.2500	0.8337
Seizure disorder	0.3333	0.7649	0.3148	0.7179
End stage or chronic renal failure	0.3273	0.8120	0.3333	0.8304
Trauma, head	0.3191	0.8677	0.2593	0.8337
Bone marrow transplant, status post	0.3158	0.8211	0.3571	0.9107
Respiratory distress, other	0.3141	0.7902	0.3774	0.7825
Renal transplant, status post	0.3077	0.9203	0.5714	0.9249
Upper airway obstruction, post-ENT surgery	0.3051	0.8627	0.2090	0.7852
Cerebral palsy	0.2899	0.8613	0.3364	0.8346
Seizures, status epilepticus	0.2885	0.7940	0.3951	0.7612
Diabetes insipidus	0.2857	0.9168	0.1111	0.8534
Hypertension, systemic	0.2778	0.8692	0.1111	0.8506
Disseminated intravascular coagulopathy	0.2759	0.8992	0.1333	0.9198
Acute lymphoid leukemia	0.2759	0.8444	0.2121	0.8466
Liver transplant, status post	0.2759	0.7974	0.4348	0.7198
Bronchiolitis due to other infectious organism	0.2667	0.9174	0.2353	0.9371
Upper airway obstruction, other	0.2366	0.8228	0.1833	0.7411
Arteriovenous malformation of the brain	0.2245	0.8428	0.2941	0.8488
Atrial septal defect	0.2222	0.8575	0.0597	0.7277
Renal disorder, unspecified	0.2182	0.7953	0.2286	0.7716
Congestive heart failure	0.2174	0.8821	0.0000	0.7842
Apnea	0.2162	0.7994	0.0000	0.7670
Acute and subacute necrosis of the liver	0.2105	0.8581	0.1961	0.7821
Sepsis, other	0.2045	0.8768	0.1500	0.8518
Trauma, vehicular	0.2029	0.8043	0.2258	0.7926
Chromosomal abnormality	0.1951	0.7958	0.2000	0.8083
Biliary atresia	0.1905	0.8750	0.5556	0.9008
Neutropenia	0.1905	0.7702	0.0816	0.7956
Hydrocephalus, congenital	0.1878	0.7177	0.1625	0.7127
Aspiration	0.1818	0.6299	0.0435	0.7183
Neurologic disorder, unspecified	0.1647	0.7191	0.0833	0.6750
Intracranial hemorrhage	0.1611	0.7327	0.1695	0.7504
Pneumothorax	0.1579	0.7746	0.0862	0.7628
Pneumonia, other	0.1505	0.8770	0.1250	0.8433
Respiratory syncytial virus	0.1500	0.9039	0.2400	0.8348
Genetic abnormality	0.1462	0.6777	0.0741	0.6483
Werdnig-Hoffman disease	0.1429	0.9737	0.0513	0.9657
Bronchopulmonary dysplasia	0.1416	0.8341	0.1081	0.8667
Pulmonary hypertension, secondary	0.1379	0.9528	0.0606	0.8942
Malignant neoplasm, gastrointestinal	0.1364	0.7748	0.0606	0.6832
Upper airway obstruction, Croup syndrome	0.1333	0.9253	0.0000	0.9376
Encephalopathy, unspecified	0.1333	0.7709	0.0921	0.7872
Prematurity (less than 37 weeks gestation)	0.1260	0.7415	0.1194	0.7031

Condition	ML-LSTM-TR, AuxOut (Diagnoses)		MLP, First 6 + Last 6	
	F1	AUC	F1	AUC
Cerebral edema	0.1250	0.8955	0.1000	0.9097
Cystic fibrosis with pulmonary manifestations	0.1250	0.8889	0.1429	0.8535
Thyroid dysfunction	0.1250	0.6381	0.0346	0.5683
Gastrointestinal surgery complication	0.1176	0.6041	0.0000	0.6495
Gastroesophageal reflux	0.1096	0.7812	0.0813	0.7746
Pneumonia, organism unspecified	0.1075	0.8283	0.1073	0.8338
Coagulopathy	0.1071	0.7543	0.0667	0.6783
Encephalopathy, hypoxic-ischemic	0.1067	0.8262	0.1429	0.8254
Hematoma, subdural	0.1039	0.8166	0.0000	0.6717
Cardiac arrest, outside hospital	0.0952	0.8712	0.1667	0.9051
Pneumonia due to inhalation of food or vomitus	0.0952	0.8114	0.1168	0.8588
Urinary tract infection	0.0952	0.7405	0.0576	0.7338
Intracranial hypertension	0.0938	0.7963	0.0690	0.7882
Ventricular septal defect	0.0923	0.6722	0.0833	0.5964
Cardiac dysrhythmia, unspecified	0.0909	0.8262	0.0513	0.7196
Drowning and non-fatal submersion	0.0909	0.7160	0.2500	0.7561
Child abuse suspected	0.0870	0.9253	0.0000	0.8455
Pneumonia due to pneumococcus	0.0811	0.8102	0.1463	0.8135
Craniofacial malformation	0.0800	0.8803	0.1429	0.8200
Shock, hypovolemic	0.0779	0.8805	0.0000	0.8951
Pneumonia due to adenovirus	0.0779	0.8015	0.2143	0.9446
Cardiomyopathy	0.0759	0.6806	0.0000	0.5084
Orthopaedic surgery complication	0.0746	0.7937	0.1290	0.8239
Infectious condition in newborn, rule out sepsis	0.0719	0.7379	0.0000	0.7269
Pleural effusion, unspecified	0.0714	0.8490	0.0879	0.8303
Malignancy of bone	0.0714	0.7127	0.1429	0.7906
Neurofibromatosis, unspecified	0.0702	0.7447	0.0439	0.7500
Trauma, blunt	0.0645	0.8790	0.0302	0.8145
Hydrocephalus, shunt failure	0.0645	0.7188	0.0000	0.6424
Diabetes mellitus, type I, stable	0.0625	0.6889	0.0270	0.7674
Hematologic, other	0.0615	0.7117	0.0517	0.7448
Pulmonary contusion	0.0606	0.8868	0.0550	0.9042
Asthma, unspecified without status asthmaticus	0.0602	0.6628	0.0000	0.6198
Thrombocytopenia	0.0600	0.6967	0.0000	0.7379
Malignant neoplasm, disseminated	0.0556	0.7063	0.0759	0.7533
Gastrointestinal disorder, unspecified	0.0556	0.6619	0.0000	0.5379
Anemia, hemolytic or other	0.0548	0.8052	0.0240	0.6400
Anemia, acquired	0.0541	0.7455	0.0755	0.7814
Spinal cord lesion	0.0541	0.6392	0.0741	0.7363
Trauma, long bone injury	0.0526	0.9087	0.0000	0.8957
Neuromuscular disorder, other	0.0522	0.6704	0.0335	0.7555
Hyponatremia	0.0506	0.7668	0.0000	0.7005
Metabolic disorder, unspecified	0.0476	0.7848	0.0000	0.6252
Obesity, unspecified	0.0471	0.6480	0.0000	0.8226
Insomnia with sleep apnea	0.0418	0.6601	0.0650	0.8345
Unspecified Intestinal obstruction	0.0408	0.6305	0.0571	0.7737
Trauma, abdominal	0.0404	0.6790	0.0435	0.6993
Congenital heart disease, unspecified	0.0397	0.7890	0.0000	0.7992
Acute Pancreatitis	0.0396	0.8179	0.1333	0.8683
Hematoma, epidural	0.0390	0.8423	0.0000	0.8278
Gastrointestinal bleed, lower	0.0385	0.6866	0.1538	0.7876
Upper airway obstruction, post-extubation	0.0377	0.7083	0.0227	0.7193
Metabolic acidosis	0.0370	0.8119	0.0000	0.8830
Gastrointestinal bleeding, upper	0.0323	0.6785	0.0513	0.7468
Neuroblastoma	0.0317	0.6430	0.0317	0.5669
Respiratory arrest	0.0303	0.7722	0.0000	0.8873
Congenital central alveolar hypoventilation syndrome	0.0294	0.7668	0.0328	0.4910
Thoracic surgery	0.0286	0.7841	0.0571	0.6843
Muscular dystrophy	0.0280	0.8763	0.1481	0.8275
Trauma, other	0.0275	0.7944	0.0000	0.8198

Condition	ML-LSTM-TR, AuxOut (Diagnoses)		MLP, First 6 + Last 6	
	F1	AUC	F1	AUC
Cardiac dysrhythmia, ventricular	0.0265	0.8629	0.0095	0.4957
Obstructed V-P shunt	0.0256	0.6769	0.0586	0.7137
Primary malignant neoplasm, Thorax	0.0247	0.6546	0.0217	0.5191
Dehydration	0.0230	0.7850	0.0000	0.7463
Hemophilus meningitis	0.0224	0.8297	0.0116	0.6643
Cardiac disease, unspecified	0.0211	0.8263	0.0000	0.7581
Panhypopituitarism	0.0205	0.8161	0.0374	0.8198
Cerebral infarction	0.0195	0.7572	0.0000	0.6236
Tetralogy of fallot	0.0185	0.7750	0.0000	0.7009
Immunologic disease, other	0.0173	0.8860	0.1111	0.7996
Cardiac dysrhythmia, supraventricular tachycardia	0.0153	0.7841	0.0952	0.8544
Trauma, chest	0.0146	0.7272	0.0571	0.8194
Pulmonary edema	0.0145	0.8113	0.0345	0.8276
Pericardial effusion	0.0115	0.7177	0.0759	0.8762
Craniosynostosis	0.0113	0.8263	0.1905	0.8778
Anemia, sickle-cell	0.0096	0.7009	0.0000	0.5136
Coma	0.0065	0.6830	0.0952	0.6799